Original paper

No differences in miRNA expression in the stroma of ERG+ and ERG– prostate cancers

Gracjan Wątor[1], Maria Kołton-Wróż[1], Paweł Wołkow[1], Łukasz Bełch[2], Piotr Chłosta[2], Joanna Szpor[3,4], Agnieszka Klimkowska[4], Katarzyna Nejman[3], Alicja Józkowicz[5], Aleksandra Piechota-Polańczyk[5], Krzysztof Okoń[3,4]

[1]Center for Medical Genomics OMICRON, Jagiellonian University Medical College, Kraków, Poland
[2]Department of Urology, Jagiellonian University Medical College, Kraków, Poland
[3]Department of Pathomorphology, Jagiellonian University Medical College, Kraków, Poland
[4]Department of Pathomorphology, University Hospital in Kraków, Kraków, Poland
[5]Department of Medical Biotechnology, Faculty of Biochemistry, Biophysics and Biotechnology, Jagiellonian University, Kraków, Poland

Prostate cancer (PC) is one of the most common cancers in males. A significant proportion of PCs bear TMPRSS2-ETS translocation and overexpress ERG transcription factor, allowing classification into ERG+ and ERG– groups, which differ in several features including the tumor microenvironment. The aim of the study was to verify whether they differ in expression of the miRNA in the microenvironment. The material consisted of 150 radical prostatectomies. Immunohistochemistry (IHC) for ERG was done using a routine method. FISH for TMPRSS2-ETS translocation was done with a ZytoLight SPEC ERG/TMPRSS2 TriCheck Probe. From each case, a representative section was selected, and tumor and non-tumor were microdissected with the LMD7000 device. RNA was isolated using the RNeasy Mini Kit system (Qiagen) and miRNA libraries were prepared with the NEBNext Multiplex Small RNA Library Prep Set for Illumina and their sequencing was performed on the NexSeq 500. Statistical analysis was done with Statistica and R software. When analyzing the expression of miRNAs some differences could be seen, but after correction for multiple comparisons was applied, these were found to be non-significant.

Key words: prostate cancer, TMPRSS2-ETS translocation, miRNA

Introduction

Prostate cancer (PC) is one of the most common cancers worldwide, with 1.4 million new cases and 375 thousand cancer-related deaths in 2020. PC is the most common cancer in men in both the Americas, western Europe, Australia, but also Japan and most of the African continent [1]. The molecular pathogenesis of PC is only partially understood, but unlike other common epithelial malignancies, a significant proportion of cases show recurrent translocation, which appears in the early stage of carcinogenesis. This translocation consists of the fusion of genes TMPRSS2 and ETS family and leads to the overexpression of transcription factors belonging to the ETS family; usually it is ERG. As ERG is easily detected at the immunohistochemical level, PC can be divided into the ERG+ and ERG– groups [2]. ERG appears to induce several features important for carcinogenesis, especially epithelial-to-mesenchymal transition and

cellular motility, and expression of genes involved in cell proliferation and invasion, while ERG– tumors are associated with increased expression of genes involved in androgen signaling [3-5]. ERG+ prostate cancers are more likely to be diagnosed at a younger age and have a higher Gleason score than ERG– tumors. ERG+ tumors are also more likely to metastasize and have a worse prognosis than ERG– tumors. ERG+ tumors have been shown to be less responsive to androgen deprivation therapy (ADT) [6].

In our previous studies, we estimated the proportion of ERG+ cases in Poland at 46%; we also revealed several differences in tumor morphology and in particular the microenvironment [7–10]. Some studies have suggested that miRNAs may influence the biology of PC, including its invasiveness and response to antiandrogen treatment [11, 12]. In the present study, our objective was to discover whether miRNA expression is similar or different in the stroma surrounding ERG+ and ERG– PC.

Material and methods

All patients underwent radical prostatectomy at the Department of Urology between 2013 and 2015. The material consisted of cases drawn from the files of the Department of Pathology. Cases with poor preservation of the tissue as assessed by optical microscopy as well cases with very small tumors, defined as present in one tissue block, were excluded from the study. All the patients from whom informed consent was obtained were included in the study. The resection specimens were formalin-fixed, and the entire prostate with spermatic vesicles was processed. From the paraffin blocks, the tissue sections were cut and stained by the hematoxylin and eosin method.

All cases were reviewed by a pathologist with experience in urologic pathology (K.O.). The grade and stage were re-assigned by the most current criteria, taking care of consistency of classification [13, 14]. Approximate prostate volume was estimated as $v = a \times b \times c \times 0.523598$, where a, b and c are the dimensions of the resected gland noted on gross examination of the specimen.

The clinical details, including PSA level, disease status (alive without evidence of disease, alive with disease, dead of disease or for unrelated causes), and date of the relapse were drawn from patients' files.

The immunohistochemistry for ERG was done on tissue microarrays, as previously described [15]. Briefly, from each case, one representative section was chosen. On the slide, the region of interest containing carcinoma tissue was marked, then its extent was copied to the surface of the paraffin block. For tissue microarray (TMA) production, a manual device (Histopathology Inc., Hungary) was used. From the region marked as cancer on each paraffin block, two 2 mm cores were obtained and transferred to a recipient block. The case numbers with respective location in the TMA were noted on an Excel (Microsoft Inc., USA) spreadsheet. The upper-left corner of the TMA was left empty to allow proper orientation of the resulting slides. From the TMA paraffin blocks, 2 μm sections were prepared for hematoxylin-eosin (HE) staining and immunohistochemistry. HE slides were used to control the quality of tissue selections. Immunohistochemistry was done in the routine manual manner. Paraffinized samples were cut into 5 μm slices using a microtome (Thermo Fisher Scientific), deparaffinized and boiled for 15 min in citric acid buffer (pH 6.0) to activate antigen, permeabilized in 0.01% of Triton X-100 for 2 min, washed, and incubated with 0.25% glycine in PBS for 30 min. Next, tissue sections were blocked for 1 h in 0.5% goat serum (GS) at room temperature. After washing in PBS, samples were incubated overnight (4°C) with anti-rabbit Nrf2 polyclonal antibodies (dilution 1 : 50 H-300, Santa Cruz) diluted in 0.5% GS. The next day, samples for Nrf2 IHC were washed and incubated with anti-rabbit HRP-conjugated antibody for 1 h at room temperature and the reaction was visualized with a DAB substrate kit (Abcam). Nuclei were counterstained with hematoxylin. Samples were analyzed under a light microscope (Nikon). The results were scored as positive when there was unequivocal nuclear staining; very faint nuclear and any cytoplasmic reactions were ignored. The results were collected in an Excel spreadsheet containing the case numbers.

The fusion status of TMPRSS2-ERG was determined using a triple-labelled color commercial probe flanking both TMPRSS2 and ERG. From each case, a representative HE section was chosen and the region of interest containing carcinoma tissue was marked on the slide. From the selected blocks, 3 μm thick tissue sections were prepared. After deparaffinization, the tissue sections were treated with a commercial Tissue Digestion Kit following the manufacturer's instructions. After tissue section pretreatment, triple-color probes ZytoLight SPEC ERG/TMPRSS2 TriCheck Probe and target DNA were co-denatured and hybridized using the automated hybridizer HYBrite (Abbott Molecular). Then post-hybridization washes were performed to remove nonspecific hybridization, and the slides were counterstained with 4,6-diamino-2-phenylindole (DAPI). The results were visualized using a fluorescent microscope (BX53, Olympus) with a ZyBlue/ZyGreen/ZyOrange Triple Bandpass Filter Set (Zytomed Systems GmbH).

Sections from the same paraffin blocks as for FISH were also used for laser microdissection, performed on an LMD7000 device (Leica). The operator first dissected the cancer cells until obtaining the quantity of material required for the nucleic acid extraction and analysis. Afterwards, the operator dissected the cells

in the stroma near the tumor infiltrate until obtaining the quantity of material required for the nucleic acid extraction and analysis. Each time 6–10 tissue sections from the region of interest were cut. The cancer and the stroma were identified by their morphology, after being prestained using the HE protocol.

After microdissection, the samples were placed on ice and then stored at –70°C until the RNA isolation was performed with the RNeasy Mini Kit system (Qiagen) and miRNA libraries were prepared with the NEBNext Multiplex Small RNA Library Prep Set for Illumina. Up to 100 ng of low-molecular weight RNA was subjected to library preparation steps: 3' adapter annealing, primer hybridization, 5' adapter annealing, reverse transcription, and finally amplification of the obtained cDNA (PCR enrichment, 14 cycles) together with the sequencing primer and the individual barcode for each sample. From the miRNA libraries ~140 bp fragments were selected by an automatic fragment separator (BluePippin) and cleaned on magnetic beads. Quality control and quantification of the libraries were performed on a TapeStation (Agilent). Library sequencing was performed on a NexSeq 500 (Illumina). Briefly, a pool of 48 samples (each with an individual tag sequence) were run at a concentration of 1.8 pM with 20% addition of the PhX artificial genome (Illumina). Sequencing was performed using a High Output Kit v.2.5 (75 cycles). The raw sequences were demultiplexed according to 6-nucleotide markers at the beginning of the sequence. Sequence quality control was performed with FastQC software; the adapters were removed with Cutadapt. All sequences below 15 nucleotides, as well as sequences lacking adapters, were removed. The cleaned sequences were paired with mirBase 22.1 [16] and counted with the miRDeep2 (Max Delbrück Center, Berlin, Germany) program. Secondary data analysis such as differential expression using edgeR [17] was previously described [18].

Statistical analysis was done with Statistica (v. 13, TIBCO Software Inc.) and R [19]. For the comparison of continuous variables, the t test was used with correction for multiple comparisons when appropriate. For comparison of qualitative variables, the χ^2 test was used. The significance level was set to 0.05.

The informed consent of all patients participating in the study was obtained. The study received the approval of the Jagiellonian University Bioethics Committee (approval 122.6120.149.2016).

Results

The material consisted of 150 cases. The mean age of the patients was 61.8 years (range 38–75, SD 6.30). Mean prostatic volume was 36.67 cm^3. The grades of the cancers are shown in Table I. The stages were pT2 in 50 cases, pT3a in 77 cases, pT3b in 22 cases and pT4 in 1 case. In 2 cases there were lymph node metastases, while in 20 cases no lymph nodes were sampled. Surgical margins were positive in 67 cases. In 58 cases vascular invasion was present. ERG status by immunohistochemistry was positive in 52 (34.4%) and negative in 99 (65.6%) cases. By FISH, ERG-

Table I. Histological grades of prostate cancer cases under study, according to current version of Gleason system and the new ISUP system (also called 'grade groups') [14]

Gleason score	Number of cases	ISUP grade	Number of cases
3+3=6	61	1	61
3+4=7	58	2	58
4+3=7	21	3	21
4+4=8	5	4	6
5+3=8	1		
4+5=9	2	5	4
5+4=9	2		

Table II. The most significant differences in miRNA expression between ERG+ and ERG– samples

miRNA	*T* statistics	*P*	*P*, corrected
hsa-miR-423-5p	–3.3169	0.0011	0.4694
hsa-miR-4488	–2.8891	0.0043	0.5563
hsa-miR-543	–2.8262	0.0052	0.5563
hsa-miR-454-3p	2.7021	0.0075	0.5563
hsa-let-7b-5p	–2.6796	0.0080	0.5563
hsa-miR-320c	–2.5670	0.0110	0.5563
hsa-miR-9-3p	2.3865	0.0180	0.5563
hsa-miR-9-3p	2.3865	0.0180	0.5563
hsa-let-7f-2-3p	2.3669	0.0190	0.5563
hsa-miR-9-3p	2.3610	0.0193	0.5563

TMPRSS2 fusion-associated deletion was detected in 31 cases, while in 82 cases these genes were unaltered. Alteration in the ERG and TMPRSS2 gene only was seen in 10 and 6 cases, respectively. In the remaining cases the FISH was not readable.

When analyzing the expression of miRNAs some differences could be seen, but after correction for multiple comparisons was applied, these resulted were found to be non-significant (Table II).

Discussion

The prognosis for organ confined PC is very good, with 5-year survival exceeding 95%, but in later stages of the disease it falls to 30%. Most new cases are diagnosed at the organ-confined stage; thus, a significant number of patients die from PC, while even a greater proportion receive an unnecessary aggressive treatment [20]. Consequently, there is a need for new methods of stratifying patients for therapy planning. Although the stage as well as histological grade remain basic prognostic factors, it has been postulated that the interaction with the tumor microenvironment may play an important role in tumor progression, and thus prognosis [21].

MicroRNAs (miRNAs) are small noncoding RNAs that play important regulatory roles in various cellular processes, including cell differentiation, proliferation, and apoptosis. At the cellular level, miRNAs influence the expression of mRNA, but also noncoding RNA sequences, including other miRNAs. This results in complicated interaction networks, which are only partially understood. Dysregulation of miRNA expression has been linked to human diseases, especially the development and progression of many types of cancer, including prostate cancer [22]. In prostate cancer, several miRNAs have been identified as either tumor suppressors or oncogenes. For example, miR-34a, miR-15a, and miR-16 are down-regulated in prostate cancer and act as tumor suppressors by targeting genes involved in cell cycle regulation and apoptosis. On the other hand, miR-21, miR-221/222, and miR-155 are up-regulated in prostate cancer and act as oncogenes by targeting tumor suppressor genes and promoting cell proliferation and survival [11, 12, 23]. Recent studies have also shown that miRNAs play a role in prostate cancer metastasis. For example, miR-101 and miR-218 have been shown to inhibit the migration and invasion of prostate cancer cells by targeting genes involved in epithelial-mesenchymal transition (EMT), a process that plays a crucial role in tumor metastasis [24, 25]. Therefore, dysregulation of miRNAs is an important factor in the development

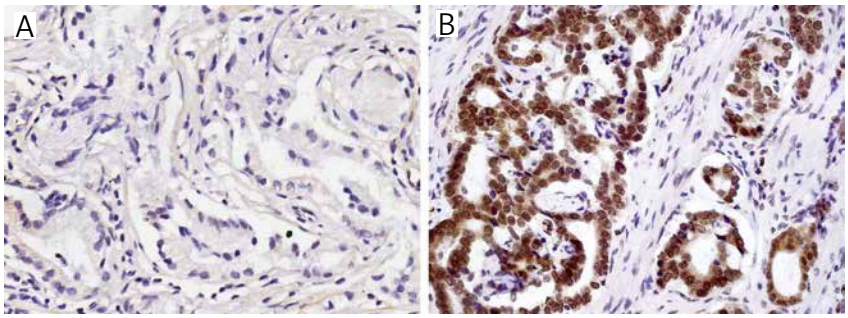

Fig. 1. ERG negative (**A**) and ERG positive (**B**) prostate cancer. Immunohistochemistry, original magnification 400×

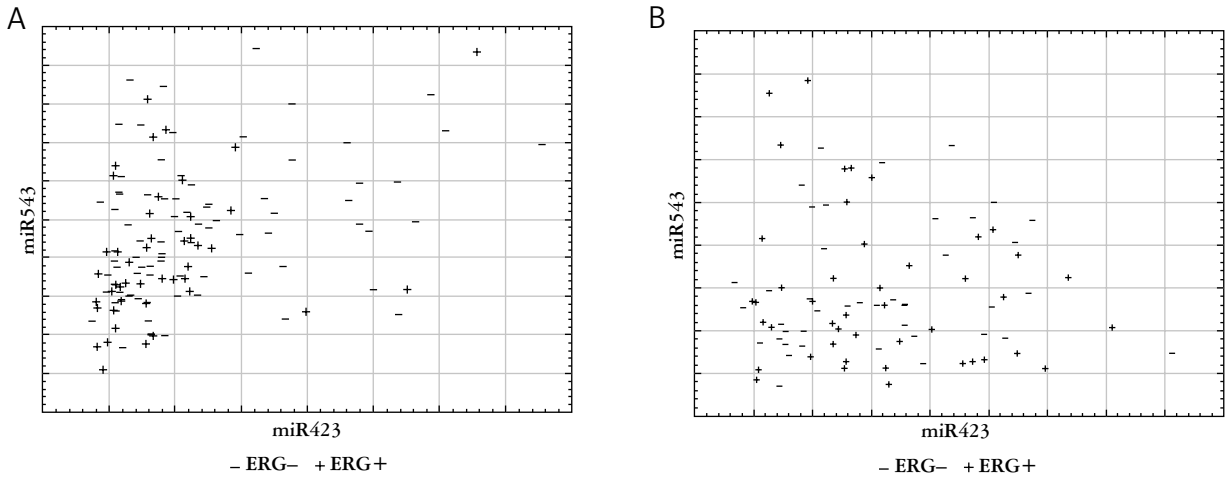

Fig. 2. Relationship of miR423 and miR543 and ERG status (**A**) and ERG-TMPRSS2 translocation status (**B**), as an example

and progression of prostate cancer, and miRNAs have potential as diagnostic and therapeutic targets for this disease. Shan *et al*. [26] reported that tumor-associated fibroblasts may secrete exosomes containing miR-423-5p, which enhance cancer cells' resistance to chemotherapy. Zhang *et al*. [27] used advanced bioinformatic tools to analyze available data from The Cancer Genome Atlas and found that several RNA molecules significantly correlated with prognosis. The aim of their study was similar to our own, as they searched for the factors influencing the microenvironment and immune response. Xie *et al.* [28] evaluated the participation of circSMARCC1 cancer-related macrophages and found up-regulation of this RNA molecule. circSMARCC1 was correlated with tumor proliferation and progression.

We previously identified several differences between the microenvironment of ERG+ and ERG– PC. In our material, the ERG+ cancers had a significantly denser microvascular network [10] and higher concentrations of FOXP3+ regulatory lymphocytes [7], mast cells [8] and other inflammatory cells [9]. Some of the differences between ERG+ and ERG– PC were observed by other authors as well [29, 30]. Some of the available data suggest that miRNA may act differently in translocation-associated and non-translocation-associated PC [31]. Kao *et al*. [32] found that members of the miR-30 family could act as intermediaries between Src and ERG and participate in epithelial-mesenchymal transition, cell proliferation, and migration. Todorova *et al*. [33] found that miR-204 negatively regulates the product of TMPRSS2/ERG fusion by increasing methylation of the TMPRSS2 promoter. In the late phase of PC evolution, miR-204 could promote C-MYC signaling, allowing the development of resistance to androgen deprivation. Zhang *et al*. [34] identified the miR-200b subfamily (miR-200a, miR-200b, miR-205, miR-429) as specifically targeted in PC translocated with TMPRSS2-ETS. This is surprising, as these miRs are known to exert a tumor suppressor effect. The authors of the cited paper thought that this paradox could explain the slow rate of PC development. According to Kim *et al.* [35] miR-200c is modulated by ERG in PC and participates in the induced epithelial-to-mesenchymal transition (EMT), cell migration, and invasion. Many miR studies have been performed on cell cultures; this allows one to control the experimental conditions and obtain precise results, but hampers any analysis of the relationship between tumor cells and their microenvironment. In our project, we aimed to provide such an analysis, but we were unable to detect differences between ERG+ and ERG– cases.

Acknowledgements

This study was supported by a grant from the National Science Centre, Poland (no. 2015/19/B/NZ5/00044) to Krzysztof Okoń.

The authors declare no conflict of interest.

References

1. Sung H, Ferlay J, Siegel RL, et al. Global Cancer Statistics 2020: GLOBOCAN estimates of incidence and mortality worldwide for 36 cancers in 185 countries. CA Cancer J Clin 2021, 71: 209-249.
2. Tomlins SA, Rhodes DR, Perner S, et al. Recurrent fusion of TMPRSS2 and ETS transcription factor genes in prostate cancer. Science 2005, 310: 644-648.
3. Wang J, Cai Y, Yu W, et al. Pleiotropic biological activities of alternatively spliced TMPRSS2/ERG fusion gene transcripts. Cancer Res 2008, 68: 8516-8524.
4. Carver BS, Tran J, Chen Z, et al. ETS rearrangements and prostate cancer initiation. Nature 2009, 457: E1; discussion E2-3.
5. Yu J, Yu J, Mani RS, et al. An integrated network of androgen receptor, polycomb, and TMPRSS2-ERG gene fusions in prostate cancer progression. Cancer Cell 2010, 17: 443-454.
6. Font-Tello A, Juanpere N, de Muga S, et al. Association of ERG and TMPRSS2-ERG with grade, stage, and prognosis of prostate cancer is dependent on their expression levels. Prostate 2015; 75: 1216-1226.
7. Kaczmarczyk-Sekula K, Galazka K, Glajcar A, et al. Prostate cancer with different ERG status may show different FOXP3-positive cell numbers. Pol J Pathol 2016; 67: 313-317.
8. Milek K, Kaczmarczyk-Sekula K, Strzepek A, et al. Mast cells influence neoangiogenesis in prostatic cancer independently of ERG status. Pol J Pathol 2016; 67: 244-249.
9. Milek K, Szpor J, Tyrak KE, et al. Lymphoid infiltrate and ERG status in prostatic carcinoma. Analytical and Quantitative Cytopathology and Histopathology 2018; 40: 183-192.
10. Strzepek A, Kaczmarczyk K, Bialas M, et al. ERG positive prostatic cancer may show a more angiogenetic phenotype. Pathol Res Pract 2014; 210: 897-900.
11. Cozar JM, Robles-Fernandez I, Rodriguez-Martinez A, et al. The role of miRNAs as biomarkers in prostate cancer. Mutat Res Rev Mutat Res 2019; 781: 165-174.
12. Abramovic I, Ulamec M, Katusic AB, et al. miRNA in prostate cancer: challenges toward translation. Epigenomics 2020; 12: 543-558.
13. Fine SW, Amin MB, Berney DM, et al. A contemporary update on pathology reporting for prostate cancer: biopsy and radical prostatectomy specimens. Eur Urol 2012; 62: 20-39.
14. Epstein JI, Egevad L, Amin MB, et al. The 2014 International Society of Urological Pathology (ISUP) Consensus Conference on Gleason Grading of Prostatic Carcinoma: Definition of grading patterns and proposal for a new grading system. Am J Surg Pathol 2016; 40: 244-252.
15. Kaczmarczyk K, Dyduch G, Bialas M, et al. Frequency of ERG-positive prostate carcinoma in Poland. Pol J Pathol 2013; 64: 175-179.
16. Griffiths-Jones S, Grocock RJ, van Dongen S, et al. miRBase: microRNA sequences, targets and gene nomenclature. Nucleic Acids Res 2006, 34: D140-144.
17. Robinson MD, McCarthy DJ, Smyth GK. edgeR: a Bioconductor package for differential expression analysis of digital gene expression data. Bioinformatics 2010, 26: 139-140.

18. Pietrus M, Seweryn M, Kapusta P, Wołkow P, Pityński K, Wątor G. Low expression of miR-375 and miR-190b differentiates grade 3 patients with endometrial cancer. Biomolecules 2021, 11: 274. DOI: 10.3390/biom11020274.
19. R Core Team: R: A Language and Environment for Statistical Computing. R Foundation for Statistical Computing; 2017.
20. Steele CB, Li J, Huang B, et al. Prostate cancer survival in the United States by race and stage (2001-2009): findings from the CONCORD-2 study. Cancer 2017; 123 Suppl 24: 5160-5177.
21. Harryman WL, Warfel NA, Nagle RB, et al. The tumor microenvironments of lethal prostate cancer. Adv Exp Med Biol 2019; 1210: 149-170.
22. Hill M, Tran N. miRNA interplay: mechanisms and consequences in cancer. Dis Model Mech 2021, 14: dmm047662. DOI: 10.1242/dmm.047662.
23. Sharma N, Baruah MM. The microRNA signatures: aberrantly expressed miRNAs in prostate cancer. Clin Transl Oncol 2019; 21: 126-144.
24. Altschuler J, Stockert JA, Kyprianou N. Non-coding RNAs set a new phenotypic frontier in prostate cancer metastasis and resistance. Int J Mol Sci 2021, 22: 2100. DOI: 10.3390/ijms22042100.
25. Wood SL, Brown JE. Personal medicine and bone metastases: biomarkers, micro-RNAs and bone metastases. Cancers (Basel) 2020, 12: 2109. DOI: 10.3390/cancers12082109.
26. Shan G, Gu J, Zhou D, et al. Cancer-associated fibroblast-secreted exosomal miR-423-5p promotes chemotherapy resistance in prostate cancer by targeting GREM2 through the TGF-β signaling pathway. Exp Mol Med 2020, 52: 1809-1822.
27. Zhang T, Wang Y, Dong Y, et al. Identification of novel diagnostic biomarkers in prostate adenocarcinoma based on the stromal-immune score and analysis of the WGCNA and ceRNA network. Dis Markers 2022, 2022: 1909196.
28. Xie T, Fu DJ, Li ZM, et al. CircSMARCC1 facilitates tumor progression by disrupting the crosstalk between prostate cancer cells and tumor-associated macrophages via miR-1322/CCL20/CCR6 signaling. Mol Cancer 2022; 21: 173.
29. Shan L, Ji T, Su X, et al. TMPRSS2-ERG fusion promotes recruitment of regulatory T cells and tumor growth in prostate cancer. Am J Med Sci 2018; 356: 72-78.
30. Kaur HB, Guedes LB, Lu J, et al. Association of tumor-infiltrating T-cell density with molecular subtype, racial ancestry and clinical outcomes in prostate cancer. Mod Pathol 2018; 31: 1539-1552.
31. Fayyaz S, Farooqi AA. miRNA and TMPRSS2-ERG do not mind their own business in prostate cancer cells. Immunogenetics 2013; 65: 315-332.
32. Kao CJ, Martiniez A, Shi XB, et al. miR-30 as a tumor suppressor connects EGF/Src signal to ERG and EMT. Oncogene 2014; 33: 2495-2503.
33. Todorova K, Metodiev MV, Metodieva G, et al. Micro-RNA-204 participates in TMPRSS2/ERG regulation and androgen receptor reprogramming in prostate cancer. Horm Cancer 2017; 8: 28-48.
34. Zhang Z, Lanz RB, Xiao LJ, et al. The tumor suppressive miR-200b subfamily is an ERG target gene in human prostate tumors. Oncotarget 2016; 7: 37993-38003.
35. Kim J, Wu L, Zhao JC, et al. TMPRSS2-ERG gene fusions induce prostate tumorigenesis by modulating microRNA miR-200c. Oncogene 2014, 33: 5183-5192.

Address for correspondence:

Krzysztof Okoń, MD, PhD
Department of Pathomorphology
Jagiellonian University, Collegium Medicum
16 Grzegórzecka St., 31-531 Kraków, Poland
e-mail: k.okon@uj.edu.pl